Journal of Engineering Science and Technology
Vol. 13, No. 10 (2018) 3129 - 3148

FREQUENCY EVALUATION FOR MECHANICAL INTEGRATION OF SHROUDED HP ROTOR BLADES IN AN AIRCRAFT ENGINE COMPRESSOR

VINAYAKA N.[1,*], NILOTPAL BANERJEE[1], B. S. AJAY KUMAR[2], KUMAR K. GOWDA[3], SURESH P. M.[4]

[1]Department of Mechanical Engineering, National Institute of Technology Durgapur, Durgapur, West Bengal 713209, India
[2]Department of Mechanical Engineering, Bangalore Institute of Technology, Bangalore, Karnataka 560004, India
[3]Department of Mechanical Engineering, Vivekananda Institute of Technology, Bangalore, Karnataka 560074, India
[4]Department of Mechanical Engineering, ACS College of Engineering, Bangalore, Karnataka 560074, India
*Corresponding Author: vn23design.engg@gmail.com

Abstract

Frequency evaluation in rotary engine blade design is an important research area because of its critical applications in aircraft engines and land-based gas engines. A compressor blade plays an important role in increasing pressure and velocity of the fluid, which influences the efficiency of gas turbines. Due to peak centrifugal stresses, gas bending loads and vibratory stresses, flow-induced blade vibrations occur leading to blade catastrophe. The airfoil is expected to prove not only the mechanical efficiency but also mechanical integrity for a desired life. The present research focuses on the study of the vibrational behaviour of an Axial HP Shrouded Compressor blade for in-service conditions. A Computational Fluid Dynamics based model is generated with reference to NACA 65-series, to analyse the flow behaviour through a linear cascade of axial compressor blades, followed by mechanical integrity stress checks to take it further with root attachment design. The present work demonstrates the need for shrouds in compressor rotor blades for stiffening the blade to avoid resonance. The positioning of the shroud is a challenge across the blade height by achieving Frequency Separation Margins using Campbell Diagram, an industry best practice.

Keywords: Blade vibrations, Campbell diagram, Frequency evaluation, Mechanical integrity, Shrouded compressor.

1. Introduction

The rotor blade of gas engine provides stiffness in opposition to steady and cyclic fluctuating loads [1] and contributes towards Mechanical Integrity. The mechanical integrity of gas engine blades can likely be achieved by ensuring vibrations at a moderate level [2]. The most challenging task in rotating machines is to accomplish the best aerodynamic and structural performance by overcoming the effects due to centrifugal force and gas bending loads [1, 3]. However, because of the wide spectrum of aerodynamic excitation, it is nearly impossible to bypass all the critical resonances in the working frequency range. High resonance stresses [4], which causes high cycle fatigue failure should be cut down to a tolerable limit. Based on a study by Afzal et al. [2], it is attained on introducing dry friction damping in rotating engine blades and occurs at contact interface in relative motion such as shroud coupling, under platform dampers, lacing wires and in the rotor blade roots in the case of the bladed disk. Compressor blade deteriorations and distortions [5] lead to a significant reduction in the gas turbine performance. Research work by Kou et al. [6] suggests that compressor blades are subjected to fatigue failure when it crosses the critical speeds during start-up and shut-down cycles. Axial flow compressors form the initials stages of all aircraft engines starting with low-pressure stages, followed by intermediate pressure stages and finally high-pressure stages, which are of prime importance. The design of axial flow compressors is a great challenge, both aerodynamically and mechanically [7] for achieving mechanical integrity. To achieve these goals generating qualified blade profiles is a pre-requisite to develop high-performance axial compressors, which is an important part of an efficient gas turbine. Air is initially accelerated by the rotor blades and then decelerated in the stator blade passages, wherein the kinetic energy transferred in the rotor is converted to static pressure [8]. This action repeats in several upcoming sections to achieve the designed overall pressure ratio.

Compressor efficiency is of prime importance in the overall performance of the gas turbine as it consumes (55-60)% of the entire power generated by gas turbine [9]. Its pressure ratio ranges from 4.15:1 to 14.6:1, for reason that the operating range needs to be between surge point and choke point. The blade platform should be a stubbed one so that it should avoid shingling. In practice, the tip clearance between the blade and the compressor casing inner surface is usually in the range of 0.5 mm to 1.5 mm. At high speeds, the possibilities of blade radial tip rub are high. It may lead to blade failure. This failure can be overcome by introducing shrouds in between the compressor rotor blades and are brought into contact by the oversize of the shrouds circumferentially or by centrifugal force, that tends to untwist the airfoil [10] as operating speed increases.

According to Rzadkowski et al. [11], introducing shroud decreases the maximal stress due to the centrifugal forces. Blade shrouding increases the high-pressure turbine 1st stage efficiency by 2-3% and decreased radial clearance by 0.8 mm [12] at main design modes, which increased efficiency by approximately 1.5%. In some cases packeted shrouded blades are used, which initiates a phase lag in the excitation acting on adjacent blades in the packet, creating less energy input and controls resonance in operating range [13]. The discontinuities of the shroud introduce asymmetry into the system, so the splitting of the modes resembles a mistuned system [11]. Shroud, though is an added mass to the blade provides additional stiffness. It is effectively placed along the blade height for high aspect-ratio rotor blades to avoid resonance, tip rubbing failure and withstands high gas

bending loads. The axial compressor design involves mean line prediction calculation through flow calculations and blade design techniques. American best practice for choosing airfoil is based on numerous families designed by the National Advisory Committee for Aeronautics (NACA), wherein the NACA 65-series is used frequently to generate the compressor blade profiles for the required performance [7].

In the present work, the gas engine HP compressor rotor blade is checked for resonance at design and off-design conditions. "Campbell Diagram" an industrial best practice tool, which is a plot of frequency vs. rotor speed along with excitations [13] and Frequency Separation Margins, are used. An ideal positioning of the shroud to avoid blade resonance is achieved along with mechanical integrity stress checks along blade height.

2. Objectives

The mechanical integrity of compressor rotor blades targets on attaining the best airfoil [1] through frequency analysis. Rotor blades are exposed to a high variation of stresses [1] in the axial compressor of a gas turbine engine. The blades experience, high gas bending loads at in-service and off-design conditions. To overcome this bending stress, the shroud is introduced in between adjacent rotor blades.

The following areas of interest are focused on the present work:

- Mechanical Integration in airfoil design with an ideal smooth transition radius to minimize [1] the localized stresses at blade hub.
- Ideal stagger angle for the compressor rotor blade for better aerodynamic performance.
- Study the role of shrouds in blade stiffening in high aspect ratio blades.
- Study the variation of sectional stress at blade hub, ¼th position, mid position, ¾th position and the tip of the blade for chosen rotor blade configurations.
- Analyse the blade Frequency Separation Margins [1, 3] and to identify the better positioning of shroud along the HP compressor rotor blade height for the design requirement.
- Develop a customized methodology for frequency evaluation in compressor rotor blade design [1].

3. Design Considerations for Achieving Mechanical Integrity

The following preliminary assumptions are considered during the design process:

- Working fluid considered is air with a mass flow rate of air as 20 kg/seconds, inlet.
- Pressure is 1.01325 bar, the inlet temperature is 301 K and tip speed is 350 m/s.
- Axial velocity C_a is 150 m/s and stage efficiency is 90.45% [5, 8].
- Pressure ratio is 4.15, hub diameter is 278 mm [8], number of stator blades are 33, number of rotor blades are 40, blade transition radius is 2 mm and angle of attack is 18^{o}.
- Factor of safety assumed is 1.68 [1] for allowable gross yield stress of 357.7689 MPa. High blade aspect ratio of 2.25, with a 81 mm blade height and 36 mm chord length.
- Over-speed rotor blade testing is assumed to be 121%, as per American Petroleum Institute (API) standards [1].

The blade material [1, 3] chosen is Titanium alloy (Ti-6Al-4V) and properties are shown in Table 1.

4. Forces Acting on an Airfoil

Figure 1 shows the forces acting on an airfoil geometry. The lift that an airfoil generates depends on the density of air, flow velocity, viscosity, the compressibility of air, the surface area of the airfoil, the shape of airfoil and angle of attack [14], which are complex parameters. Thus, they are characterized by a single variable in the lift equation called the lift coefficient [15]. The lift equation [15] is given by Eq. (1):

$$L = \frac{1}{2}\rho V^2 S C_L \tag{1}$$

Figure 2 shows that for 16˚ to 18˚ angle of attack, maximum lift coefficient is obtained, which is 1.70.

Table 1. Ti-6Al-4V mechanical properties [1, 3].

	Value	Unit
Coefficient of thermal expansion	9.7e-6	/℃
Young's modulus	1.138e5	N/mm^2
Poisson's ratio	0.342	-
Yield strength	880	N/mm^2
Density	4.43e-9	Tonnes/mm^3

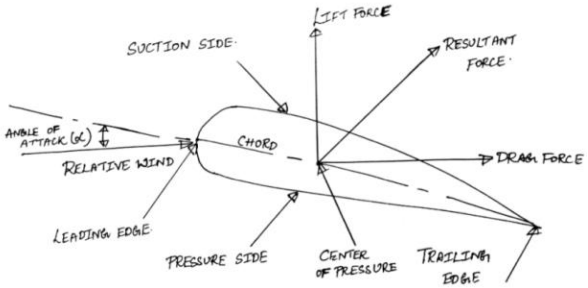

Fig. 1. Schematic representation of forces acting on an airfoil.

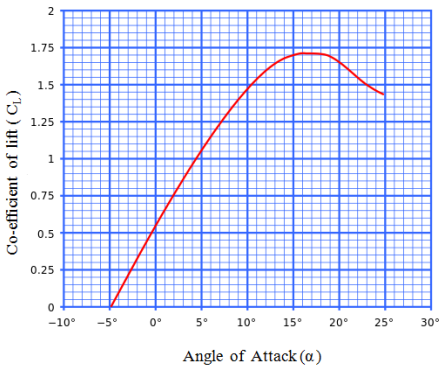

Fig. 2. Coefficient of lift (C_L) vs. angle of attack (α) [16].

5. Compressor Rotor Blade Configurations

Figures 3(a) and (b) show the finite element model along with a number of nodes and elements for No Shroud Blade Model and blade model with a shroud at 3/4th position along the blade height of a HP compressor rotor. Initially, an airfoil is generated using Computational Fluid Dynamics, for the desired HP compressor stage. Later, the model is fine-meshed using higher order TET-10 element [1] and subjected to structural analysis.

To carry out comparative case studies of frequency evaluation for NSBM and for various shrouded HP compressor rotor blade configurations of a gas engine, modal analysis is performed. This is to achieve better structural integrity without any resonance at operating speeds and at 121% over-speed conditions of the gas engine. For the frequency analysis, a total of 5 cases of rotor blade configurations are modelled and subjected to modal analysis [1] in ANSYS commercial package, for frequency evaluation at design and off-design conditions.

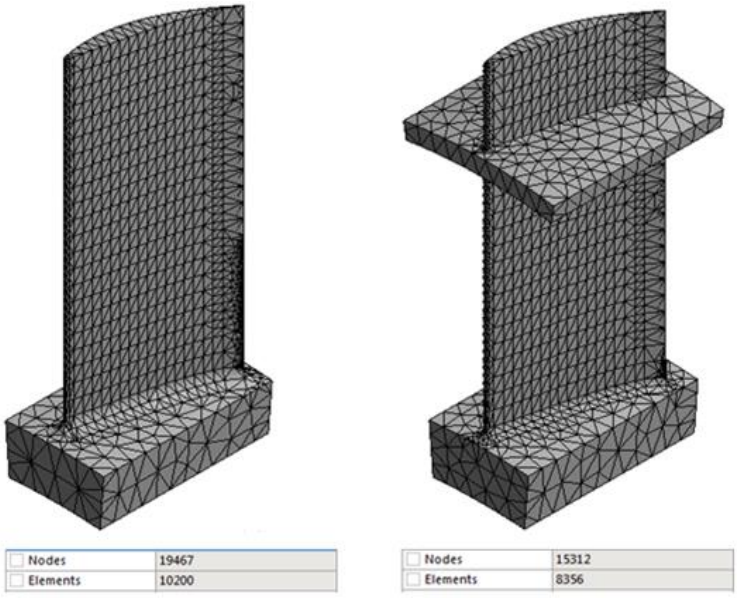

(a) NSBM. **(b) 0.75 SBM.**

Fig. 3. Meshed model of compressor rotor blade configurations.

6. Vibration Characteristics of an Aero Engine Axial Compressor

Design of more efficient rotor blades of an axial compressor stage of a gas turbine is more critical than a turbine stage, as it is exposed to diverse fluctuating loads and wake flow excitations [1]. The axial compressor is the initial foundation for the succeeding combustor and turbine sectors. Hence, the structural and overall efficiency of axial compressor blades, play an important role in a gas turbine total performance [1].In turbo-machine blade design, the computation of blade natural frequencies is very influential, as blade failure due to fatigue develops at resonant frequencies [1, 17]. Hence, investigation of vibration characteristics plays a significant role in designing turbo-machines [1, 3].

7. Mode Shape Identification and Separation Margin Evaluation [1]

The rotor blade without a shroud is a cantilever beam. In engineering practice, the initial 3 mode shapes namely 1st bending, 1st flip and 1st torsion are chosen as critical modes for evaluation. However, all the first 8 modes need to be free from resonance, with sufficient separation margin ranging from 5% to 10% from operating speed.

Excitations 1*X* to 8*X* (*X*= *N*/60), is considered as critical for the wake forces leaving the airfoil for the analysis [1]. Figure 4 shows the first 3 mode shapes of a shrouded blade model with a shroud at a 3/4th position along blade height and a free standing blade without the shroud.

Campbell Diagram is plotted for all the calculated rotational speeds. More attention is taken up towards the first 3 modes of vibration, due to the powerful excitations that come out for the first 8 engine orders [1]. If acceptable separation margins are not attained, the blade experiences resonance and is subjected to high cycle fatigue. Therefore, frequency tuning of the initial 3 modes with a greater margin of safety becomes important [1].

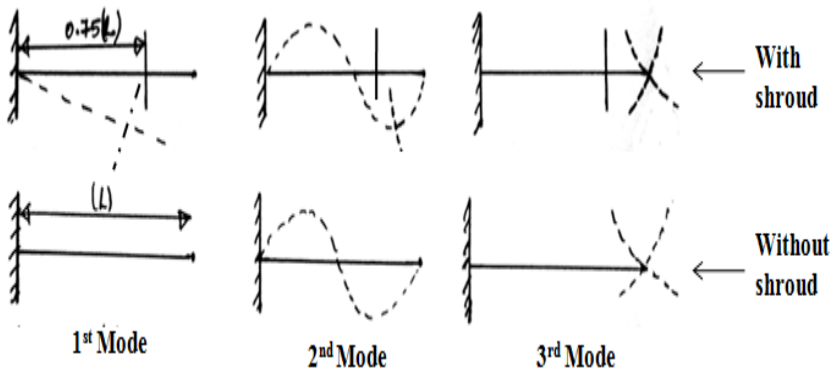

Fig. 4. First 3 modes of cantilever blade vibration with shroud and without shroud at 0.75 position along blade length.

8. Test Cases Considered

The following are the test cases taken up for the present research:

- Computational Fluid Dynamic (CFD) analysis for blade stagger angle variations from 2° to 18°.
- Frequency Evaluation by Campbell Diagram (CD) for NSBM of height 81 mm followed by Analysis of Frequency Separation Margins [1] in the Exciter Box for chosen 81 mm NSBM.
- Comparison of average sectional stress at various positions along blade height from hub to tip for chosen compressor rotor blade configurations.
- Frequency evaluation by Campbell Diagram (CD) for chosen 81 mm shrouded compressor rotor blade configurations.
- Comparison of mode 1 frequency of chosen compressor rotor blade configurations at 100% operating speed.

8.1. CFD analysis for blade stagger angle variations from 2° to 18°

Stagger angle is the angle made by the chord line of blade airfoil with the axial direction of the gas turbine and is also termed as setting angle. Studies reveal that for a stagger angle of 0 and 25 deg., the conducted general numerical experiments demonstrates that, damping of slant shroud coupling is certainly more than the zig-zagging [18]. An experiment on gas turbine cascade in off-design condition signifies that small deviations in stagger angle will lead to notable variation in cascades performance [19]. The stagger angle increase weakens the tip vortex and moves it downstream slightly because the blade loading is decreased [20, 21]. Hence, to reduce eddies, the stagger angle is varied from 2^{o} to 18^{o} and CFD analysis is performed.

8.1.1. Grid and boundary conditions

Figure 5 shows a Hexahedral grid generated for the periodic sectors considered in the analysis. The total grid count is 147,000 nodes. Inlet mass flow rate and the total temperature is applied as the inlet boundary condition. Exit static pressure is applied as the exit boundary condition. The speed of 15000 rpm is applied as the rotational speed for the rotor with a hub-tip ratio of 0.475, for the present research work. Figure 6 shows a variation of hub-tip ratio vs. speed in rpm of the compressor rotor. Periodic steady-state analysis is performed with stage interface applied between the stationary and rotating components. Shear Stress Transport (SST) turbulence model is considered for this Computational Fluid Dynamic analysis and the blade is staggered from 2° to 18°, to get the ideal flow over an airfoil.

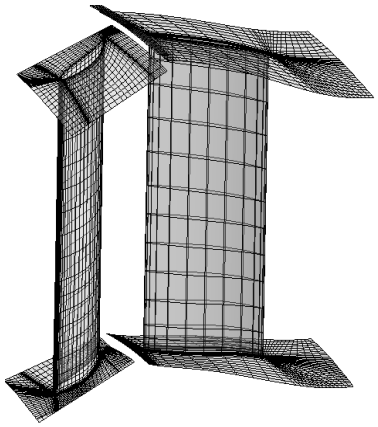

Fig. 5. Grid generated for the compressor blades.

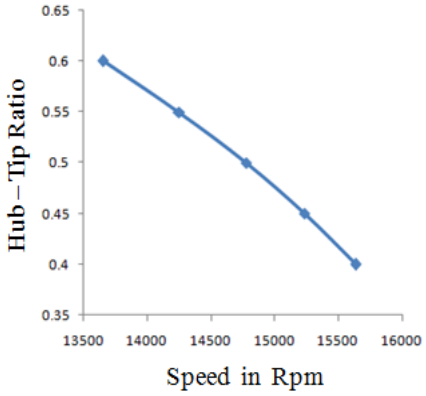

Fig. 6. Variation of rotor blade hub-tip ratio vs. rotor speed in rpm [8].

8.1.2. Velocity distribution for 2° stagger angle

From Fig. 7, it is observed that the fluid is re-circulating more in compressor blades for 2° stagger angle at the $3/4^{th}$ position when compared to $1/4^{th}$ and 1/2 position along blade height, which is not acceptable as this create eddies, which obstructs the flow and hence, reduces the stage efficiency. Hence, the same procedure is followed by varying the stagger angle from 2° to 18° minimize this re-circulation and to get better streamlines.

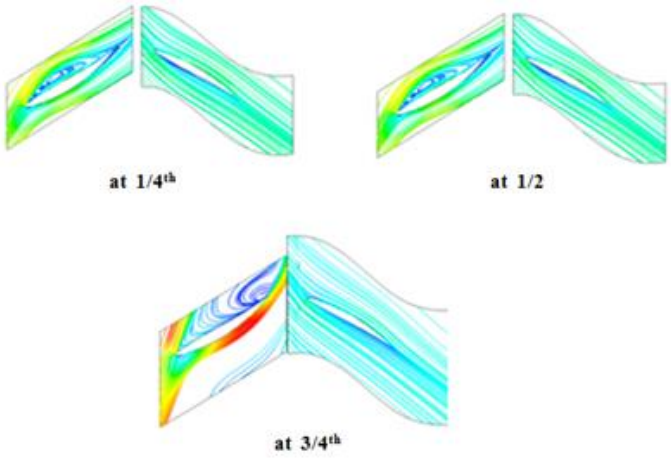

Fig. 7. Velocity distribution along blade height for 2° stagger angle.

8.1.3. Velocity distribution for 6° stagger angle

From Fig. 8, it is observed that the fluid is still re-circulating to a greater extent in compressor blades for 6° stagger angle at the 3/4th position when compared to 1/4th and 1/2 position along blade height, but it shows a bit improvement in streamlines when compared to in 2° stagger angle case.

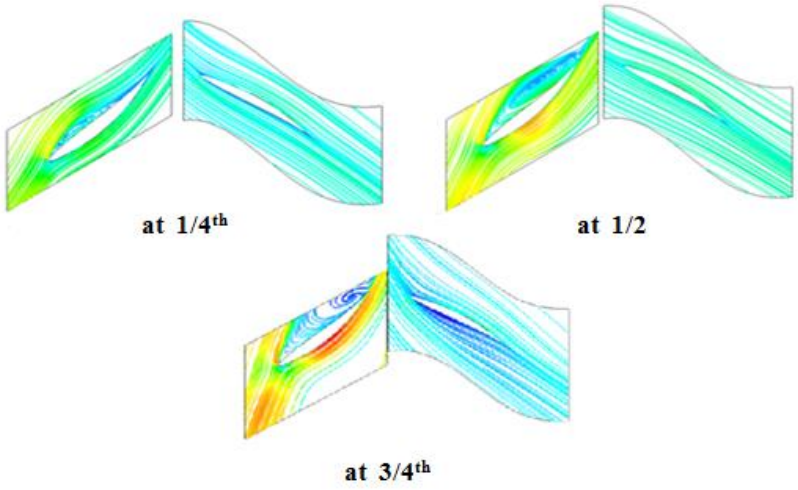

Fig. 8. Velocity distribution along blade height for 6° stagger angle.

8.1.4. Velocity distribution for 18° stagger angle

From Fig. 9, it is observed that blades with stagger angle of 18° provides smoother streamlines at all sections, i.e., at 1/4th, 1/2 and 3/4th position along blade height, when compared to that of 2° and 6° and stagger angle test cases. Hence, blades are now set to a stagger angle of 18° and are further subjected to structural analysis.

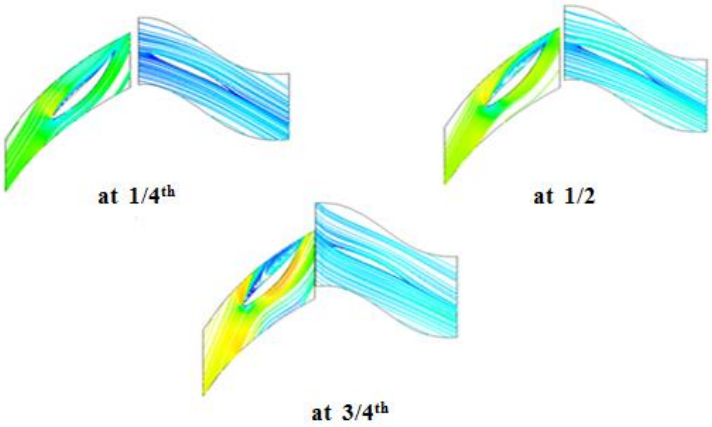

Fig. 9. Velocity distribution along blade height for 18° stagger angle.

8.2. Frequency evaluation of 81 mm NSBM configuration

In the present section, NSBM configuration without any shroud is subjected to modal analysis and blade frequencies are obtained for speeds ranging from zero to over-speed conditions and Campbell Diagram and Exciter Box are plotted for detailed blade frequency evaluation.

8.2.1. Campbell diagram (CD) for 81 mm NSBM

Figure 10 shows the Campbell Diagram results obtained for NSBM of 81 mm blade height. Campbell Diagram indicates that Mode 1 frequency is crossing over with the 3*X* excitation within the operating zone. However, Mode 2 and Mode 3 frequencies are excited by higher order engine excitations, which carry less importance in exciting the blade with high impact. Since the higher order excitations are weak, the best practice is to address the first 8 engine orders, due to its chances of high potential to excite the blade under service conditions. It should satisfy even at 121% over-speed condition as per requirement of API standards [1]. Hence, it paves the way for the further detailed analysis of Frequency Separation Margins and Mode excitations [1] evaluation, for the highlighted region through the Exciter Box for Mode 1.

8.2.2. Analysis of frequency separation margins (FSM) in the exciter box [1] for 81 mm NSBM

Figure 11 is the Exciter Box, illustrating a detailed representation of the 2*X* to 4*X* excitations passing near the Mode 1 frequency for the considered engine operating speed separation margins range from 95% to 121%, derived from a selected highlighted region in Campbell Diagram of Fig. 10. From the Fig. 11, it is observed that 3*X* excitation line clearly undergoes resonance as highlighted in the considered separation margin [1] regions, for 100% operating speed of 15000 rpm for Mode 1 frequency line, which leads to blade failure. Also, the industry best practice requires that the minimum first 3*X* excitations should pass below the Mode 1 natural frequency line, which is not satisfied by 81 mm NSBM as seen in Fig. 10. Hence, in the present case, it is compulsory to shift the Mode 1 frequency to a higher engine order, for better structural performance. The Mode 1 frequency can be moved to higher excitations either by

introducing a twist in the blade or by providing shrouds. Therefore, in the case of HP blades, it would be a good practice to introduce shroud with or without cover bands, to tune the blade for improved resonance conditions.

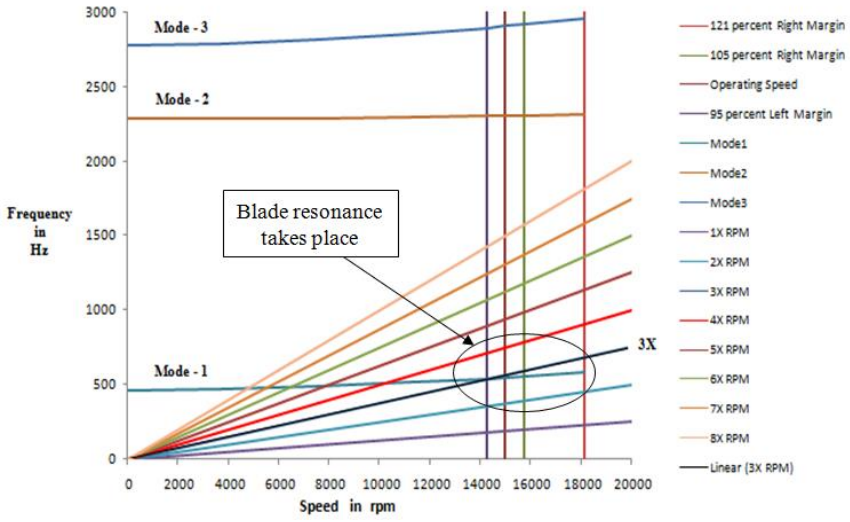

Fig. 10. CD for 81 mm NSBM.

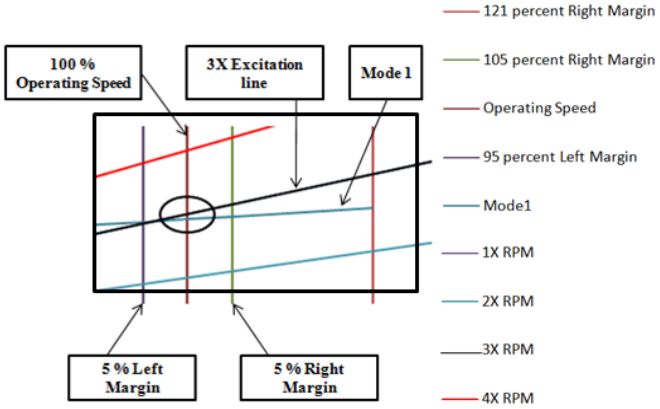

Fig. 11. Exciter Box for 81 mm NSBM.

8.3. Comparison of average sectional stress at various positions along blade height from hub to tip for chosen compressor rotor blade configurations

To increase the structural stiffness of 81 mm NSBM and simultaneously for achieving greater separation margins for safe operating zones and to avoid blade resonance, there is a need for structural blade inter-connecting element called "Shroud" to be introduced in between rotor blades, perpendicular to blade height. No doubt the shroud serves effectively to increase the blade stiffness, but on the contrary it is an extra mass to be added to the blade; hence, it calls for further

investigation that where exactly these shrouds need to be positioned along blade height, for better mechanical integrity and to overcome blade failures in high aspect ratio rotor blades.

Hence, before performing frequency evaluation, sectional stress checks are carried out at the blade hub, 1/4th position, mid-span, 3/4th position and the tip of the blade for both no shroud and with-shroud blade models, for the chosen 81 mm height of blade, to determine, which rotor blade configuration is the best at an operating speed of 15000 rpm. These sectional stresses should always meet the requirement, that it should be less than the gross yield stress of the rotor blade of 357.7689 MPa.

Figure 12(a) shows the average sectional stress at blade hub for 81 mm NSBM, which is around 134.95 MPa and Fig. 12(b) shows the average sectional stress at blade tip for 81 mm 0.75 SBM, which is around 0.80751 MPa. Both the stress values are well within gross yield stress of 357.7689 MPa.

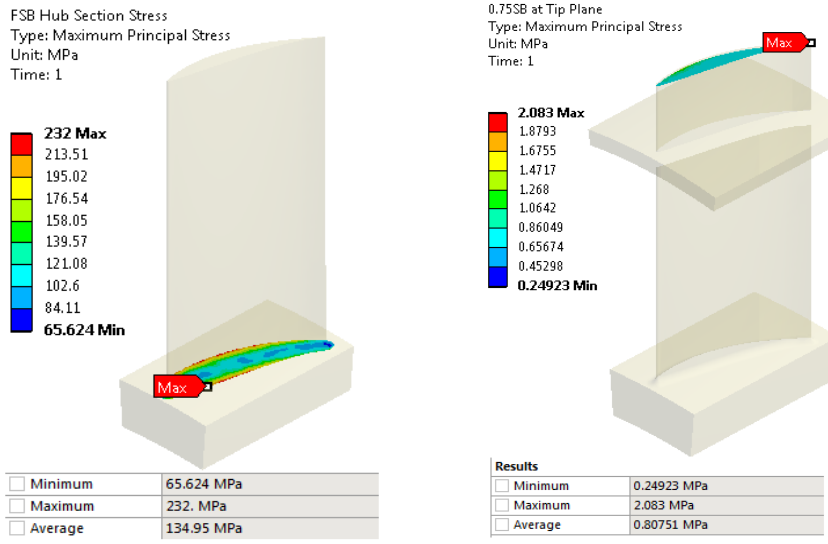

(a) NSBM. **(b) 0.75 SBM.**

Fig. 12. Sectional stress plots for 81mm blade height.

From the knowledge-based engineering, it is said that the rotor blade behaves like a cantilever beam, as its stubbed platform is assumed to be in 100% fixity condition with rotor disc. The rotor blade upon loading should show that maximum stress is at the fixed end that is at blade hub [10] and minimum stress should be at the blade tip. So, stress should gradually decrease from the blade hub to blade tip. Here, NSBM case results are neglected, as there is a need to provide additional stiffness to the blade by introducing shrouds in between the rotor blades.

Figures 13 and 14 results show that, there is a close competition to choose the best configuration among the rotor shrouded blade configurations considered and upon comparing values for blade hub and blade tip case, it infers that 0.25 SBM gives the best mechanical integrity at blade hub, with least average sectional stress

of 137.32 MPa and 0.75 SBM provides the best mechanical integrity at blade tip, with least average sectional stress of 0.80751 MPa.

Thus, there is a need for further investigation to decide, which one is the best configuration, among the rotor, shrouded blade configurations considered. This can be finally concluded through frequency evaluation by using Campbell Diagram.

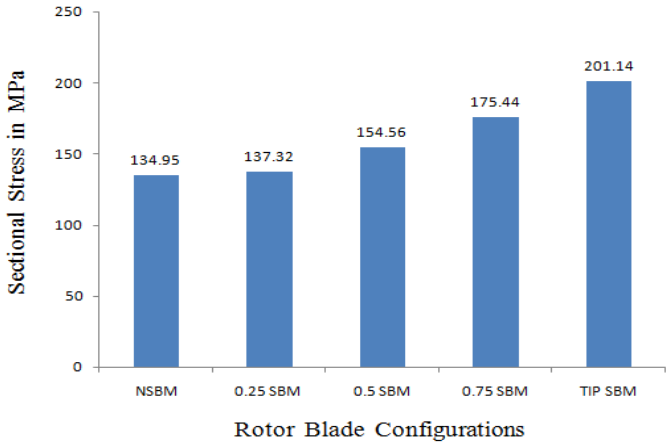

Fig. 13. Comparison of sectional stress at blade hub for 81 mm blade height.

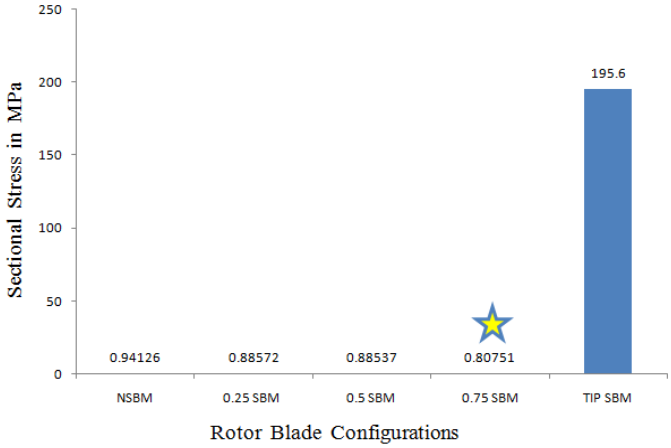

Fig. 14. Comparison of sectional stress at blade tip for 81 mm blade height.

8.4. Frequency evaluation by campbell diagram (CD) for chosen 81 mm shrouded compressor blade configurations

Shrouding is effective when the bladed disk is excited in resonance or close to resonance [21]. Figures 15 to 18 shows the Campbell Diagrams plotted for 0.25 SBM, 0.5 SBM, 0.75 SBM and TIP SBM respectively, for frequency analysis at the design and off-design operating conditions. On introducing shrouds, all the shrouded compressor rotor blade configurations, have their respective 3*X* excitation lines passing below their Mode 1, with an acceptable margin, which is one of the

basic requirement. Figure 15 shows that 0.25 SBM undergoes resonance due to the intersection of the 4*X* and 5*X* excitation line with Mode 1 frequency line, as highlighted at 121% over-speed condition and close to 95% speed respectively. Hence, 0.25 SBM is not recommended. Figure 16 of 0.5 SBM infers that 8*X* excitation line undergoes resonance at 120% over-speed condition as highlighted at off-design speeds. Hence, 0.5 SBM is not recommended as the rotor blade should be safe at both design and off-design conditions. Whereas, Figs. 17 and 18 show that all 8*X* excitation lines pass safely without any resonance condition and are well within Mode 1 frequency line, for the chosen engine operating speed separation margins range from 95% to 121%. Hence, now it is necessary to choose the best blade configuration, which provides the highest blade stiffness, among the remaining two blade configurations, i.e., 0.75 SBM and TIP SBM. This can be found out by plotting a comparative graph of Mode 1 frequency, for the chosen compressor rotor blade configurations.

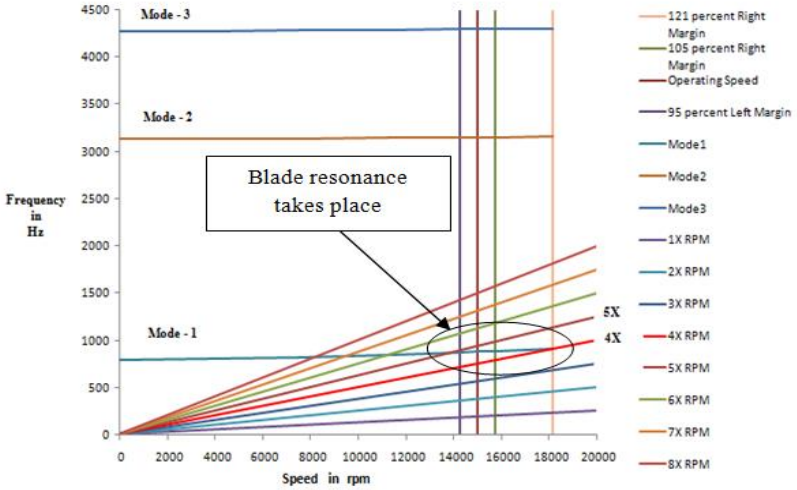

Fig. 15. CD of 81 mm, 0.25 SBM.

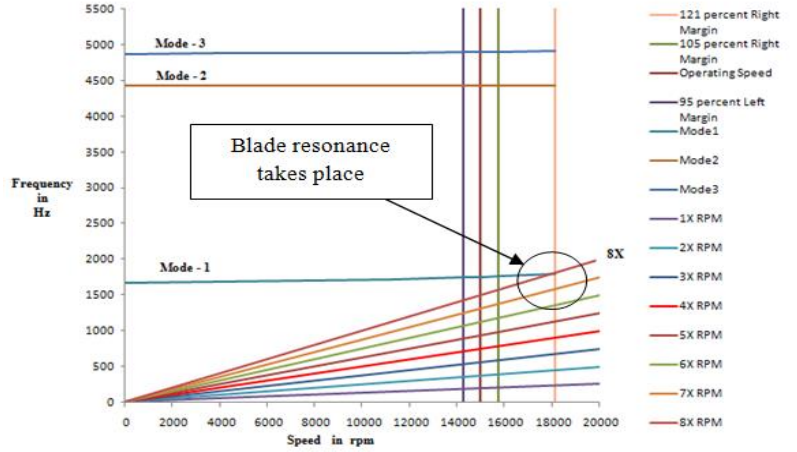

Fig. 16. CD of 81 mm, 0.5 SBM.

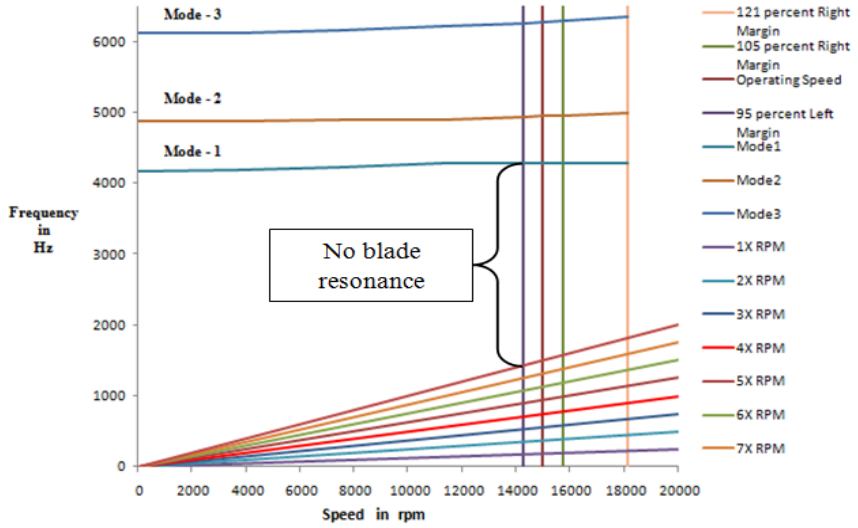

Fig. 17. CD of 81 mm, 0.75 SBM.

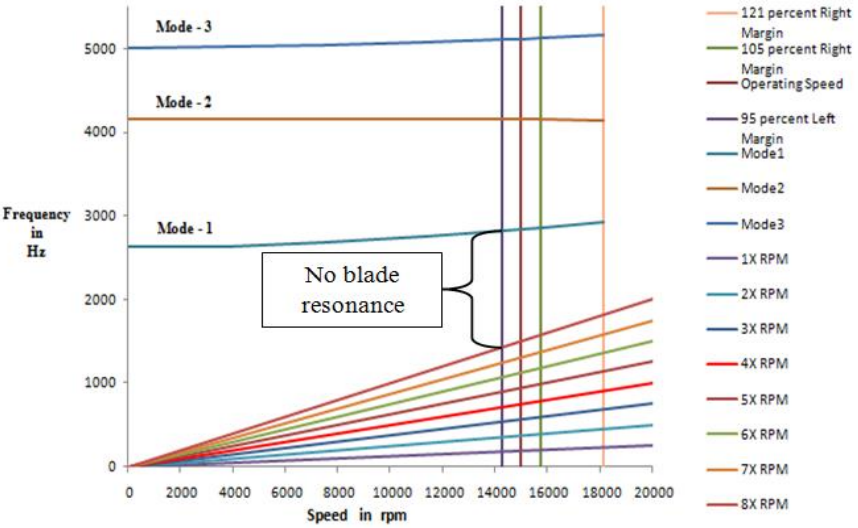

Fig. 18. CD of 81 mm, TIP SBM.

8.5. Comparison of mode 1 frequency of chosen compressor rotor blade configurations at 100% operating speed

Figure 19 shows the plot of Mode 1 natural frequency, for the chosen compressor rotor blade configurations at 100% operating speed. From comparative graph Fig. 19, it clearly concludes that 0.75 SBM provides the highest Mode 1 natural frequency of 4288.4 Hz, whose value is greater than Mode 1 natural frequency of 2834.8 Hz provided by TIP SBM configuration, which is its close competitor. Hence, it can be concluded that 0.75 SBM provides the highest stiffness and is the better suitable compressor rotor blade configuration in an Aero-Engine rotor.

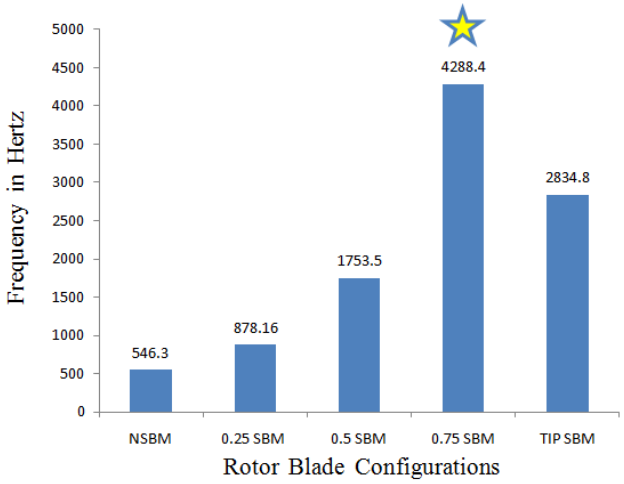

Fig. 19. Comparison of Mode 1 frequency of chosen rotor blade configurations.

9. Comparison of Theoretical Calculations and Modal Analysis Results for Mode 1 Frequency for Chosen Rotor Blade Configurations

9.1. Theoretical calculations for Mode 1 frequency

The considered blade is of airfoil cross-section [22] in nature as shown in Fig. 20.

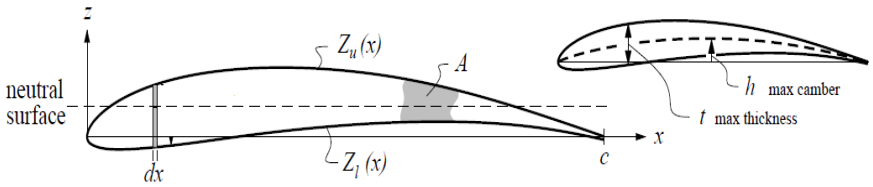

Fig. 20. Quantities for determining bending inertia of an airfoil section [22].

The formulae [22] for computing the moment of inertia and cross-sectional area, are given by:

$$t = max\{Z_u(x) - Z_l(x)\} = 3.938215 - 0.3155625 = 3.6226525\ mm \quad (2)$$

$$h = max\left\{\frac{Z_u(x) + Z_l(x)}{2}\right\} = max\left\{\frac{3.938215 + 0.3155625}{2}\right\} = 2.126889\ \text{mm} \quad (3)$$

$$T \cong \frac{t}{c} \cong 100.6292 \times 10^{-3} \quad (4)$$

$$\in \cong \frac{h}{c} \cong 59.08025 \times 10^{-3} \quad (5)$$

$K_I \cong 0.036$ and $K_A \cong 0.6$ for most common airfoils [22].

$c = 36$ mm

$$I \cong K_I c^4 T(T^2 + \in^2) \cong 82.8531\ mm^4 \quad (6)$$

$$A \cong K_A c^2 T \cong 78.2492\ mm^2 \quad (7)$$

It is observed that all the 8 powerful engine order excitations 1*X*, 2*X*, 3*X*,....8*X* pass well within the Mode 2 frequency line for the considered blade configurations, from their respective Campbell Diagram. Hence, for the validation of frequency results, only Mode 1 frequency for each blade configuration is computed theoretically. Since blade root is fixed, assuming blade to be a cantilever beam and a continuous system, the natural frequency expression [23] is given by:

$$f_n = \frac{(\beta_i\, l)^2}{2\pi} \times \sqrt{\frac{E\ \ I}{\rho\ \ A\ \ {l_e}^4}} \tag{8}$$

where $(\beta_i\, l)$ is a constant whose value for i = 1, i.e., $(\beta_1\, l)$=1.8751 [23], for Mode 1 vibration (1st bending mode), in the case of a cantilever beam. Hence, on substituting the values in Eq. (8) and computing for Mode 1 natural frequency, we get:

$f_{n_1} =$ 444.8183 Hz, for NSBM, having effective blade length, l_e= 81 mm.
$f_{n_1} =$ 790.7881 Hz, for 0.25 SBM, having effective blade length,
l_e = (1- 0.25)× 81 = 60.75 mm.

Similarly, the Mode 1 natural frequency is computed for 0.5 SBM, 0.75 SBM and TIP SBM and their values are tabulated in Table 2.

Table 2. Mode 1 frequency comparison.

Type of blade configuration	Theoretical calculation result in Hz	ANSYS result in Hz	Error in %
NSBM	444.8183	462.08	3.7357
0.25 SBM	790.7881	793.87	0.3882
0.5 SBM	1779.2732	1675.10	5.8548
0.75 SBM	3468.4305	4173.40	16.8919
TIP SBM	2830.4533	2620.40	7.4212

Table 2 gives the comparative results and error % computations, performed for theoretical calculations and modal analysis results obtained from ANSYS commercial package (sample results shown in section 9.2), for the chosen 5 compressor rotor blade configurations. The obtained results show close proximity with each other and are in acceptable range.

9.2. Modal analysis results obtained from ANSYS for Mode 1 (1st bending) frequency for NSBM and 0.25 SBM

Figures 21(a) and (b) show that, Mode 1 frequency for NSBM is 462.08 Hz and for 0.25 SBM is 793.87 Hz respectively.

10. Effect of Shroud, an Extra Mass added to the Blade

The extra mass at each cantilever blade added by shroud at each disk sector put together is treated as a continuous ring, which expands along with the blade due to centrifugal force. Tip shroud is not advisable, because we expect zero stress at the blade tip. Mid-span shroud tends to push the blade center of gravity towards its hub and hence, reduces the centrifugal force to some extent, but blade bending still prevails as remaining upper half portion of the blade is exposed to high varying gas

bending loads. In the present case, since the blade center of gravity is above mid-span as observed from geometry, it was decided to go for shroud at a 3/4th position along blade height and also from CFD it is noticed that there are fewer re-circulations at the 3/4th position for 18° stagger angle and fetched least sectional stress at the blade tip. However, shroud thickness is a criterion, which has been verified by taking section stresses in the blade from hub to tip, whose results have proven to be less than the expected gross yielding stress of blade. Shroud helps in retaining the chattering of blades during blade vibrations at higher disk modes. In order to prevent this, the shroud is introduced to protect the rotor blades from bending stress, crossing over to each other, shingling in blade platform and impact damage in the blades at a high mass flow rate for designed service life. In addition, it can be seen from Fig. 19 that an added shroud mass increases Mode 1 frequency, providing extra bandwidth, additional stiffness and prevents the blade from early resonance, based on shroud positioning. Further to this, to summarize there is a need for shrouded blades in gas engine HP compressor rotors, with a little compromise on the shroud mass added to the blade mass and its effect is taken care during the structural design.

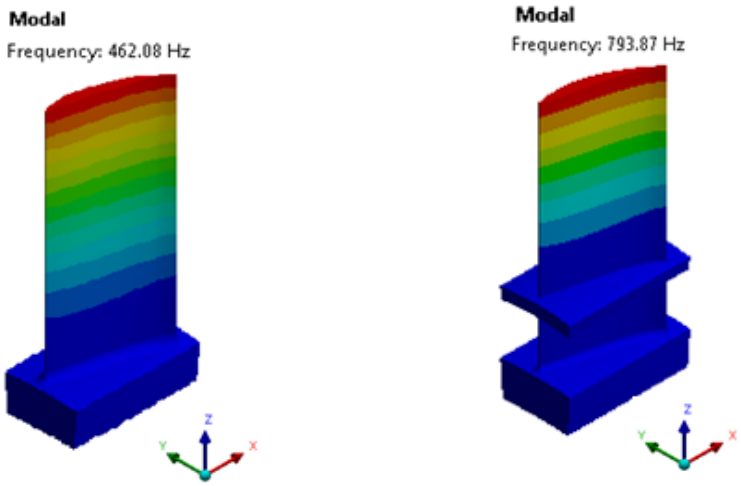

(a) NSBM. **(b) 0.25 SBM.**

Fig. 21. Mode 1 frequency of NSBM and 0.25 SBM.

11. Conclusions

Following outcomes are noticed at each stage of design:

- Mechanical Integration in airfoil design with smooth transition radius of 2 mm, to minimize localized stresses to 175.44 MPa at blade hub is achieved well within the gross yield strength [1] of 357.7689 MPa, for Ti-6Al-4V compressor HP rotor blade.
- It is found that compressor blades with a stagger angle of 18°, provide smoother streamline flows for a better aerodynamic performance of the blade without any eddies.
- Introducing shrouds to free standing rotor blade leads to increase in the natural frequency of the blades, providing greater Frequency Separation Margins and

additional stiffness to blades and achieving a separation margin of 5% to 10% from operating speed. It is observed from Campbell Diagrams of shrouded blade configurations that, the first three excitations passed as desired below the Mode 1 frequency line.

- 0.75 SBM provides a better mechanical integrity at blade root and tip, compared to other compressor HP rotor blade configurations considered.
- Figures 10, 11, 15 and 16 concludes that NSBM, 0.25 SBM and 0.5 SBM are under resonance condition for the considered 95% left margin to 121% over-speed frequency separation margin, as per American Petroleum Institute (API) standards.
- 0.75 SBM provides the highest Mode 1 natural frequency of 4288.4 Hz, when compared to other compressor rotor blade configurations considered and its value is about 7.8498 times greater than the Mode 1 natural frequency provided by NSBM at 100% operating speed.
- A customized methodology for frequency evaluation in HP compressor rotor blades in an aircraft engine is achieved and it is found that shroud at 3/4th position along rotor blade height provides highest blade stiffness among the chosen blade configurations at both design and off-design conditions.

Nomenclatures

A	Cross-sectional area of airfoil along blade length, mm^2
C_L	Lift coefficient
c	Chord length of blade, mm
E	Young's modulus, N/mm^2
h	Maximum camber, mm
I	Moment of inertia of airfoil, mm^4
K_A	Proportionality coefficient of airfoil cross-section area
K_I	Proportionality coefficient of airfoil moment of inertia
L	Lift force, N
l	Actual length of engine blade, mm
l_e	Effective length of engine blade, mm
N	Blade rotational speed, rpm
S	Area of the airfoil, m^2
T	Chord ratio
t	Maximum thickness of airfoil, mm
V	Relative velocity of the airflow, ms^{-1}
X	Running speed harmonics, rps
$Z_l(x)$	Value of co-ordinate along z axis in lower surface of airfoil corresponding to $Z_u(x)$ obtained from geometry (Fig. 20), mm Running speed harmonics, rps
$Z_u(x)$	Maximum value of co-ordinate along z axis in upper surface of airfoil obtained from geometry (Fig. 20), mm

Greek Symbols

α	Angle of attack, deg.
β_i	Roots of natural frequency expression
ε	Camber ratio

ρ	Density of air, tonnes/mm^3

Abbreviations

0.25 SBM	1/4th Position Shroud Blade Model
0.5 SBM	1/2 Position Shroud Blade Model
0.75 SBM	3/4th Position Shroud Blade Model
CD	Campbell Diagram
EB	Exciter Box
FSM	Frequency Separation Margins
NSBM	No Shroud Blade Model
TIP SBM	Tip Position Shroud Blade Model

References

1. Nagarajaiah, V.; Banerjee, N.; Ajay Kumar, B.S.; and Gowda, K.K. (2016). Aero structure interaction for mechanical integration of laced LP compressor blades in a gas engine rotor. *Proceedings of the ASME Power Conference*. Charlotte, North Carolina, United States of America, 9 pages.
2. Afzal, M.; Arteaga, I.L.; and Kari, L. (2016). An analytical calculation of the Jacobian matrix for 3D friction contact model applied to turbine blade shroud contact. *Computers and Structures*, 177(C), 204-217.
3. Vinayaka, N.; Banerjee, N.; Ajay Kumar, B.S.; and Gowda, K.K. (2016). Aero-structure interaction for mechanical integration of HP compressor blades in a gas engine rotor. CAD/CAM, robotics and factories of the future. *Lecture Notes in Mechanical Engineering*, 807-819.
4. Afzal, M.; Arteaga, I.L.; and Kari, L. (2018). Numerical analysis of multiple friction contacts in bladed disks. *International Journal of Mechanical Sciences*, 137, 224-237.
5. Lebele Alawa, B.T.; Hart, H.I.; Ogaji, S.O.T.; and Probert, S.D. (2008). Rotor blades profile influence on a gas turbines compressor effectiveness. *Applied Energy*, 85(6), 494-505.
6. Kou, H.j.; Lin, J.-s.; Zhang, J.-h.; and Fu, X.(2017). Dynamic and fatigue compressor blade characteristics during fluid-structure interaction: Part I-Blade modelling and vibration analysis. *Engineering Failure Analysis*, 76, 80-98.
7. Ujjawal, A.J.; and Joshi, S.J. (2013). Design and analysis of stator, rotor and blades of the axial flow compressor. *International Journal of Engineering Development and Research*, 1(1), 24-29.
8. Saravanamutto, H.I.H.; Rogers, G.F.C.; and Cohen, H. (2011). *Gas turbine theory (5th ed.)*. New Delhi: Dorling Kindersley (India) Pvt. Ltd.
9. Boyce, M.P. (2002). *Gas turbine engineering hand book (2nd ed.).* Houstan, Texas: Gulf Professional Publishing.
10. Wang, J.H.; and Yau, H.L. (1990). Design of shroud interface-angle to minimize the forced vibration of blades. *Proceedings of International Gas Turbine and Aeroengine Congress and Exposition*. Brussels, Belgium, 9 pages.
11. Rzadkowski, R.; Kwapisz, L.; Drewczynski, M,; Sczepanic, R.; and Rao, J.S. (2007). Free vibrations analysis of shrouded bladed discs with one loose blade. *Task Quarterly*, 10(1), 83-95.

12. Mamaev, B.I.; Petukhovsky, M.M.; and Pozdnyakov, A.V. (2013). Shrouding the first blade of high temperature turbines. *Proceedings of the ASME Turbine Blade Tip Symposium*. Hamburg, Germany, 6 pages.
13. Nagababu, P.; Krishna, T.S.S.R.; and Naveen, M.V. (2017). Frequency failure investigation on shrouded steam turbine blade through dynamic analysis. *International Journal of Innovative Research in Science, Engineering and Technology*, 6(8), 16440-16446.
14. Kandwal, S.; and Singh, S. (2012). Computational fluid dynamics study of fluid flow and aerodynamic forces on an airfoil. *International Journal of Engineering Research and Technology*, 1(7), 1-8.
15. Sullivan, A. (2010). Aerodynamic forces acting on an airfoil. Retrieved May 6, 2010, from http://physics.wooster.edu/JrIS/Files/Sullivan_Web_Article.pdf.
16. Botag. (2006). Lift curve of SM701 airfoil showing the relationship between angle of attack and lift coefficient. Retrieved April 4, 2006, from https://zh.wikipedia.org/wiki/File:Lift_curve.svg.
17. Rao, J.S. (1994). *Turbomachine blade vibration (1st ed.*). New Delhi, India: New Age International Pvt. Ltd.
18. Szwedowicz, J.; Visser, R.; Sextro, W.; and Masserey, P.A. (2007). On non-linear forced vibration of shrouded turbine blades. *Journal of Turbomachinery*, 130(1), 9 pages.
19. Zhang, W.; Zou, Z.; Pan, S.; Liu, H.; Zhou, Y.; and Li, W. (2010). Impact of stagger angle non uniformity on turbine aerodynamic performance. *Journal of Thermal Science*, 19(5), 465-472.
20. Yoon, Y.S.; Song, S.J.; and Shin, H.-W. (2006). Influence of flow coefficient, stagger angle and tip clearance on tip vortex in axial compressors. *ASME Journal of Fluids Engineering*, 128(6), 1274-1280.
21. Pennacchi, P.; Chatterton, S.; Bachschmid, N.; Pesatori, E.; and Turozzi, G. (2011). A model to study the reduction of turbine blade vibration using the snubbing mechanism. *Mechanical Systems and Signal Processing*, 25(4), 1260-1275.
22. Drela, M. (2006). Area and bending inertia of airfoil sections. Retrieved March 20, 2006, from https://ocw.mit.edu/courses/aeronautics-and-astronautics/16-01-unified-engineering-i-ii-iii-iv-fall-2005-spring-2006/systems-labs-06/spl10b.pdf.
23. Rao, S.S. (2007). *Vibration of continuous systems (1st ed.).* Hoboken, New Jersey: John Wiley & Sons, Inc.